The influence of non-radiative energy transfer on the excitation and decay of excited states of Er^{3+} in $Cs_2NaErCl_6$

1994 J. Phys.: Condens. Matter 6 1593

(http://iopscience.iop.org/0953-8984/6/8/017)

J. Phys.: Condens. Matter 6 (1994) 1593–1602. Printed in the UK

The influence of non-radiative energy transfer on the excitation and decay of excited states of Er^{3+} in $Cs_2NaErCl_6$

W Ryba-Romanowski, G Dominiak-Dzik and S Gołąb

Institute of Low Temperature and Structure Research, Polish Academy of Sciences, Okólna 2, 50-950 Wrocław 2, BO Box 937, Poland

Received 20 July 1993, in final form 30 September 1993

Abstract. Evidence for efficient non-radiative energy transfer between erbium ions in $Cs_2NaErCl_6$ is provided by excitation and luminescence spectra and luminescence lifetimes. In one of the cross relaxation schemes the excitation of the $^4F_{3/2}$ level is transferred almost exclusively to the $^4F_{9/2}$ level in the 50–300 K temperature region. The process of cross relaxation which removes the excitation from the $^4S_{3/2}$ level is switched thermally at about 100 K and attains high efficiency at room temperature. Experimental results are interpreted using previously reported energies of normal vibrations of $ErCl_6^{3-}$ and the crystal-field levels of $Cs_2NaErCl_6$. It has been noted that virtually all efficient energy transfer schemes in $Cs_2NaLnCl_6$ reported thus far involve transitions between multiplets of the ground terms of lanthanides. All these transitions obey the selection rules for magnetic dipole transitions.

1. Introduction

Lanthanide ions (Ln^{3+}) in cubic hexachloroelpasolites $Cs_2NaLnCl_6$ are situated in the crystal field of perfect octahedral symmetry and are well separated by Na–Cl–Na chains. In such a structure the pure electric dipole transitions cannot contribute to the intensities of the 4f–4f transitions, which are dominated by magnetic dipole and electric dipole vibronic transitions. Single crystals of $Cs_2NaLnCl_6$ have been considered as simple model systems, useful for testing the theoretical considerations regarding the crystal-field levels and optical absorption and emission intensities of Ln^{3+} ions. In numerous works the crystal-field energy levels have been calculated and successfully fitted to experimental levels [1–5]. Also, the intensity calculations account reasonably well for the observed vibronic and magnetic dipole intensities.

Considerably less attention has been paid to energy transfer processes and luminescence phenomena in this lattice. Weak concentration quenching of Nd^{3+} luminescence in $Cs_2NaNdCl_6$ has been reported and attributed to the large separation between neodymium ions [6, 7]. In subsequent work an efficient concentration quenching of luminescence originating in the $^1G_4$ level of Tm^{3+} in Cs_2NaYCl_6:Tm^{3+} has been noted [8]. Recently, a more systematic investigation of energy transfer between lanthanide ions in doped Cs_2NaYCl_6 crystals has been reported [9, 10] but the nature of the transfer mechanism is still not fully understood.

In the present work we report on the effect of non-radiative energy transfer on the excitation and relaxation of several excited levels of Er^{3+} in $Cs_2NaErCl_6$. We do not intend to establish a detailed mechanism of interaction between lanthanide ions in this lattice because the energy level structure of Er^{3+} is too complex. This problem poses a special challenge to the theory, since the results obtained during the investigation of the

0953-8984/94/081593+10$19.50

more simple $Cs_2NaEuCl_6$ are not fully understood [10]. The goals of this work are to provide new experimental evidence that the rates of energy transfer in $Cs_2NaLnCl_6$ may be as high as those in low-symmetry crystals, and to correlate particularly efficient energy transfer schemes reported for this system. The phenomena considered are of considerable technological interest since they influence the efficiency of luminescent materials based on lanthanides.

Energy levels of $Cs_2NaErCl_6$ and the normal vibrations of the $ErCl_6^{3-}$ moiety reported previously [5] will be used to discuss the experimental data. The scope of the work is restricted to the phenomena of excitation and relaxation of the $^4S_{3/2}$, $^4F_{9/2}$, $^4I_{9/2}$, $^4I_{11/2}$ levels, which are well separated and relatively easy to deal with. An assignment of the luminescence spectra of $Cs_2NaErCl_6$ has been proposed previously [13].

2. Experimental

Single crystals of hexachloroelpasolites were grown at 850 °C in evacuated quartz ampoules by the Bridgman method. Details of preparation and crystal growth are described elsewhere [4]. Two samples have been investigated in this study. The stoichiometry of the first one is $Cs_2NaErCl_6$ and that of the second is $Cs_2NaEr_{0.2}Yb_{0.4}Y_{0.4}Cl_6$. Additionally one single-crystal sample of composition $Cs_2NaNd_{0.4}Yb_{0.6}Cl_6$ has been grown and used as a reference for the analysis of the experimental data.

Absorption spectra were measured with a Varian Model 2300 UV–vis–NIR spectrophotometer. Excitation spectra were measured with a SPF 500 SLM Aminco spectrofluorometer. Luminescence spectra were excited by the 488 nm or 514 nm lines of an argon-ion laser, resolved by a Zeiss Model GDM 1000 double-grating monochromator and detected by a photomultiplier with S-1 or S-11 response, depending on the spectral region. Decay curves of luminescence were recorded using an apparatus comprising a nitrogen laser-pumped tunable dye laser, a prism monochromator and a SRS 250 Boxcar integrator.

For low-temperature measurements the samples were placed in an Oxford Model CF 1204 continuous flow helium cryostat equipped with a temperature controller. The sample temperature was controlled within ±1 K and the exactitude of the lifetime measurements is estimated to be 20%.

3. Results

The lifetimes and the spectra of luminescence originating in the $^4S_{3/2}$, $^4F_{9/2}$, $^4I_{9/2}$ and $^4I_{11/2}$ levels of Er^{3+} in $Cs_2NaErCl_6$ and in $Cs_2NaEr_{0.2}Yb_{0.4}Y_{0.4}Cl_6$ have been measured in the 5–295 K temperature region. The excitation spectra of the $^4F_{9/2}$ and $^4I_{11/2}$ levels have been measured at room temperature. Experimental results obtained from these measurements are shown in figures 1 to 4, and in figure 5 we present a scheme of the energy levels involved in the optical transitions. The energy level scheme has been constructed using the data for Er^{3+} in $Cs_2NaErCl_6$ given in [5].

The room temperature luminescence spectrum resulting from the excitation of the $^2H_{11/2}$ or $^4F_{7/2}$ levels is dominated by an intense band centred at 12 320 cm^{-1} and corresponding to the $^4I_{9/2}$–$^4I_{15/2}$ transition of Er^{3+}. The intensities of the $^4S_{3/2}$–$^4I_{15/2}$ and $^4S_{3/2}$–$^4I_{13/2}$ transitions centred at 18 180 cm^{-1} and 11 600 cm^{-1}, respectively, are lower by several orders of magnitude in $Cs_2NaErCl_6$ and roughly by a factor of ten in $Cs_2NaEr_{0.2}Yb_{0.4}Y_{0.4}Cl_6$. With decreasing temperature the intensity of luminescence originating in the $^4S_{3/2}$ level grows

steadily, whereas the intensity of the $^4I_{9/2}$ emission decreases and attains negligible levels at about 80 K. The evolution of the spectrum is exemplified in figure 1, which shows the luminescence bands recorded at 80 K and at 295 K, corresponding to the $^4S_{3/2}$–$^4I_{13/2}$ and $^4I_{9/2}$–$^4I_{15/2}$ transitions of Er^{3+} in $Cs_2NaErCl_6$. In figure 2 the luminescence lifetimes of the $^4S_{3/2}$ and $^4I_{9/2}$ levels are plotted versus temperature for both the samples. The weak temperature dependence of the $^4I_{9/2}$ lifetime indicates that the disappearance of this emission at low temperature is due to inefficient excitation rather than to luminescence quenching. In figure 3 the excitation spectra of the $^4F_{9/2}$ luminescence for both the samples are compared and the absorption of Er^{3+} in $Cs_2NaErCl_6$ is given as a reference. Efficient emission from the $^4F_{9/2}$ level in a diluted sample may be obtained only by direct excitation of this level. Excitation into a band centred at about 25 970 cm^{-1}, corresponding to the $^4I_{15/2}$–$^4G_{11/2}$ transition, leads to weak luminescence originating in the $^4F_{9/2}$ level, which is populated probably by the vibronic $^4G_{11/2}$–$^4F_{9/2}$ transition. In a concentrated sample an intense red emission associated with the $^4F_{9/2}$–$^4I_{15/2}$ transition results from excitation into the band which dominates the excitation spectrum (figure 3(*b*)) and corresponds to the $^4I_{15/2}$–$^4F_{5/2}$, $^4F_{3/2}$ transition. The efficiency of this excitation channel is surprisingly high and weakly influenced by temperature in the 5–300 K temperature region. Apparently, almost all the excitation of the $^4F_{5/2}$ level is transferred to the $^4F_{9/2}$ level, as no luminescence originating in the excited level nor in the other lower lying level can be detected. It has been found that the sample temperature weakly influences the $^4F_{9/2}$ lifetime, which increases from 5.51 ms at room temperature to 7.0 ms at 5 K.

In contrast to the $^4F_{9/2}$ level, no excitation channels with high efficiency have been found in the case of the $^4I_{11/2}$ level. At low temperatures the $^4I_{11/2}$ level is populated probably by vibronic transitions from excited levels higher than $^4F_{9/2}$ and the resulting luminescence is weak. At about 120 K the intensity of the $^4I_{11/2}$–$^4I_{15/2}$ emission centred at 10 000 cm^{-1} starts to grow and the decay curves of luminescence can be recorded. In the 130–300 K temperature region the excitation of the $^4S_{3/2}$ or higher level leads to decay curves of the form exemplified in figure 4. In this figure the experimental data are indicated by asterisks and the full curve represents a fit to the equation

$$I(t) = A\exp(-k_2t) + B[\exp(-k_2t) - \exp(-k_1t)] \tag{1}$$

where constant $A = 127$, constant $B = 3661$, $k_1 = 139\ s^{-1}$ is an inverse of the $^4I_{9/2}$ luminescence lifetime given in figure 2, and $k_2 = 126\ s^{-1}$ is a fitted inverse of the $^4I_{11/2}$ luminescence lifetime.

Based on the good quality of the fit we may suppose that the $^4I_{11/2}$ level of Er^{3+} in $Cs_2NaErCl_6$ is populated by direct radiative vibronic transitions from the $^4S_{3/2}$ excited level and by multiphonon emission from the $^4I_{9/2}$ level. The radiative $^4S_{3/2}$–$^4I_{11/2}$ transition dominates at low temperatures. At room temperature the cross relaxation process depletes the $^4S_{3/2}$ excitation quickly, therefore the radiative transition may contribute solely to the initial stage of population build-up in the $^4I_{11/2}$ level. The emission spectrum centred at 10 000 cm^{-1} was expected to be different in $Cs_2NaEr_{0.2}Yb_{0.4}Y_{0.4}Cl_6$ since the energy of the $^2F_{5/2}$ level of Yb^{3+} is very close to that of the $^4I_{11/2}$ level of Er^{3+} and the $^4I_{11/2}$ excitation may be transferred non-radiatively to ytterbium. As can be seen in figure 6 this expectation is confirmed by experiment. The emission spectrum at 10 000 cm^{-1} obtained with $Cs_2NaEr_{0.2}Yb_{0.4}Y_{0.4}Cl_6$ and the emission spectrum of Yb^{3+} in $Cs_2NaNd_{0.4}Yb_{0.6}Cl_6$ are identical, indicating that the excitation of the $^4I_{11/2}$ level of Er^{3+} in the sample codoped with erbium and ytterbium is transferred to ytterbium and emitted from the $^2F_{5/2}$ level.

Experimental data presented in figures 1–4 and in figure 6 are evidence that rare-earth ions, well separated and situated in the crystal field of octahedral symmetry which forbids

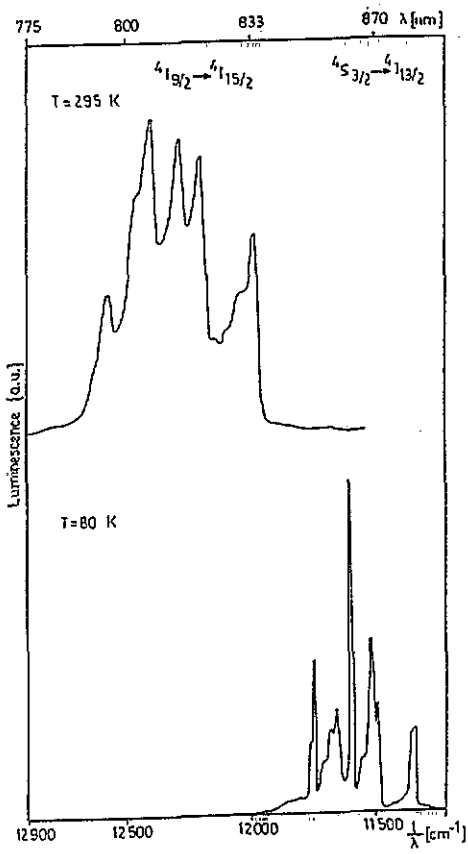

Figure 1. Luminescence bands recorded at 295 and at 80 K, corresponding to the $^4I_{9/2}$–$^4I_{15/2}$ and $^4S_{3/2}$–$^4I_{13/2}$ transitions of Er^{3+} in $Cs_2NaErCl_6$.

electric dipole transitions, may interact as efficiently as in low-symmetry crystals. In the following we will examine more closely the available data, which may help us to understand why certain excited states interact more strongly than others.

4. Discussion

In figure 5 we present an energy level scheme for Er^{3+} in $Cs_2NaErCl_6$. Radiative transitions observed in this work are indicated by full arrows. The two pairs of broken arrows indicate the non-radiative transitions involved in the processes of cross relaxation already discussed.

A significant concentration quenching of luminescence originating in the $^4F_{9/2}$ and $^4I_{11/2}$ levels is not expected since the energies of the lower-lying levels are such that no cross relaxation scheme may be constructed. Consistently, the measured lifetimes of these levels are fairly long in a concentrated sample. Concentration quenching of luminescence, originating in the $^4S_{3/2}$ level, is well documented. In most erbium-doped materials the cross

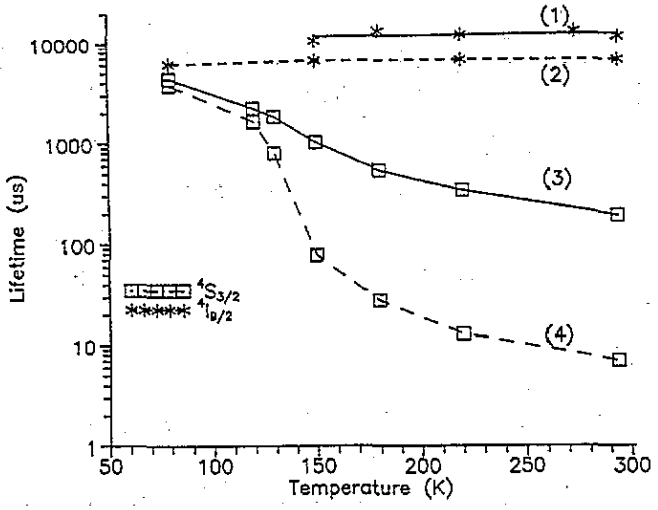

Figure 2. The influence of temperature on the luminescence lifetimes of the $^4S_{3/2}$ and $^4I_{9/2}$ levels of Er^{3+} in $Cs_2NaErCl_6$ (curves (2) and (4)) and $Cs_2NaEr_{0.2}Yb_{0.4}Y_{0.4}Cl_6$ (curves (1) and (3)).

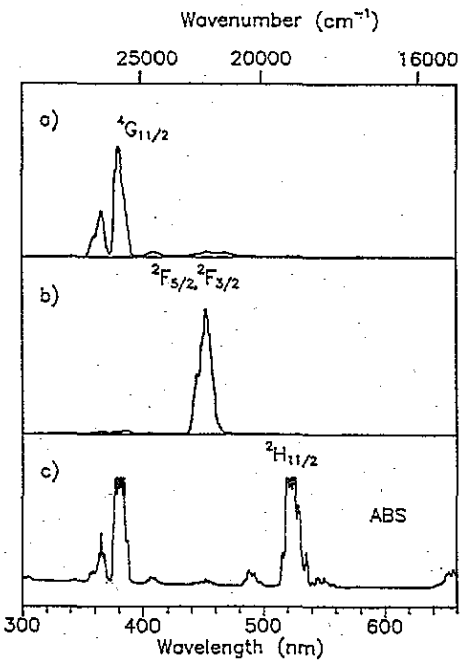

Figure 3. The excitation spectrum of the $^4F_{9/2}$–$^4I_{15/2}$ emission recorded at 300 K for (*a*) $Cs_2NaEr_{0.2}Yb_{0.4}Y_{0.4}Cl_6$, and (*b*) $Cs_2NaErCl_6$. For a comparison the absorption spectrum of $Cs_2NaErCl_6$ is shown (*c*).

relaxation scheme

$$^4S_{3/2}(\text{site1}) + {}^4I_{15/2}(\text{site2}) \rightarrow {}^4I_{9/2}(\text{site1}) + {}^4I_{13/2}(\text{site2})$$

meets the condition of resonance, with the inclusion of a phonon, and effectively dissipates the $^4S_{3/2}$ excitation.

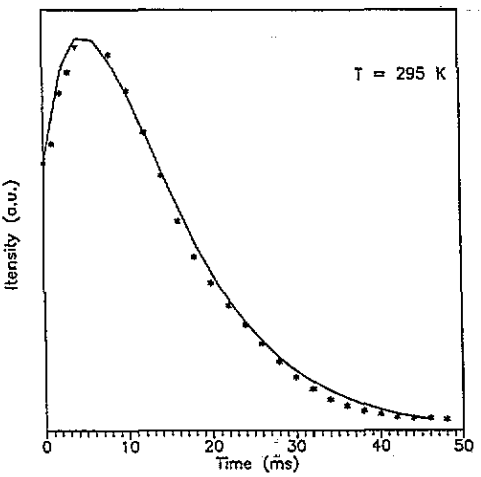

Figure 4. The time evolution of luminescence from the $^4I_{11/2}$ level of Er^{3+} in $Cs_2NaErCl_6$ following the excitation of the $^2H_{11/2}$ level. Experimental data are indicated by asterisks. The full curve represents a fit to equation (1).

The $^4I_{9/2}$ level is also prone to decay through the $^4I_{13/2}$ level according to the scheme

$$^4I_{9/2}(\text{site1}) + {}^4I_{15/2}(\text{site2}) \rightarrow {}^4I_{13/2}(\text{site1}) + {}^4I_{13/2}(\text{site2})$$

but in the majority of hosts this method of relaxation competes with an efficient multiphonon relaxation to the $^4I_{11/2}$ level, which is separated from the $^4I_{9/2}$ level by less than 2000 cm^{-1}.

Experimental data in figure 2 indicate that the luminescence from both the $^4S_{3/2}$ and $^4I_{9/2}$ levels is quenched, but in a very different manner. The energy of the unsplit $^4S_{3/2}$ level of Er^{3+} in $Cs_2NaErCl_6$ has been measured to be 18 276 cm^{-1} [5]. Three crystal-field components of the $^4I_{9/2}$ level have never been located experimentally, probably because the $^4I_{15/2}$–$^4I_{9/2}$ transition is extremely weak. The calculated values are as follows: 12 352 cm^{-1} ($a\Gamma_8$), 12 464 cm^{-1} (Γ_6), and 12 522 cm^{-1} ($b\Gamma_8$) [5].

We recorded the $^4I_{15/2}$–$^4I_{9/2}$ absorption band at 5 K with an 11 mm long $Cs_2NaErCl_6$ crystal and we made an assignment using the calculated energies given above, together with reported energies of odd-parity normal vibrations of $ErCl_6^{3-}$, namely $\nu_3(t_{1u})$ = 245–260 cm^{-1}, $\nu_4(t_{1u})$ = 107–114 cm^{-1} and $\nu_6(t_{2u})$ = 85–90 cm^{-1} [4, 5]. It can be seen in figure 7 and in table 1 that the calculated values are perfectly consistent with experimental data.

Five crystal-field levels of the $^4I_{13/2}$ multiplet have been located experimentally at 6492 cm^{-1} (Γ_6), 6517 cm^{-1} ($a\Gamma_8$), 6532 cm^{-1} ($a\Gamma_7$), 6660 cm^{-1} ($b\Gamma_8$) and 6683 cm^{-1} ($b\Gamma_7$) [5]. Only two crystal-field levels of the ground $^4I_{15/2}$ multiplet have been observed, namely Γ_7 at 25 cm^{-1} and $b\Gamma_8$ at 90 cm^{-1} above the ground $a\Gamma_8$ level. The energies of the Γ_6 and $c\Gamma_8$ levels have been calculated by several workers. The values 252 cm^{-1} and 282 cm^{-1} for Γ_6 and 283 cm^{-1} and 308 cm^{-1} for $c\Gamma_8$ have been reported [3, 5]. With these data the condition of resonance for the $^4S_{3/2}$ relaxation scheme is fulfilled solely when the downward transition is assisted by phonon absorption and the upward transition is made from the highest crystal-field levels of the ground multiplet. Such a process implies a strong temperature dependence of transfer probability and is not contradictory to experimental results. Taking into account the timescale of the plots of lifetime versus temperature in

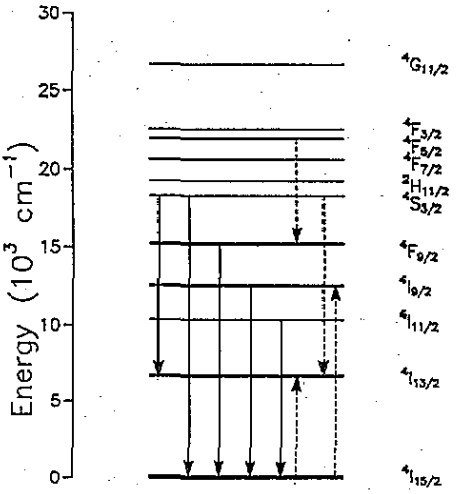

Figure 5. The energy level scheme for Er^{3+} in $Cs_2NaErCl_6$. Full arrows indicate radiative transitions. Broken arrows indicate transitions involved in the cross relaxation processes.

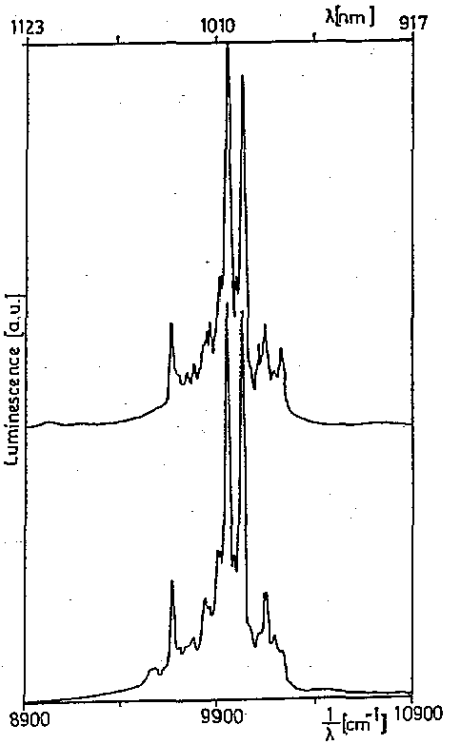

Figure 6. A comparison of the luminescence band recorded with $Cs_2NaEr_{0.2}Yb_{0.4}Y_{0.4}Cl_6$ (lower) to the luminescence band associated with the $^2F_{5/2}$–$^2F_{7/2}$ transition of Yb^{3+} in $Cs_2NaNd_{0.4}Yb_{0.6}Cl_6$ (upper). $T = 77$ K.

figure 2 we may suppose that the decrease of the $^4S_{3/2}$ lifetime in the concentrated sample is due solely to the cross relaxation. Consistently, the inverse of lifetime will approximate the concentration quenching rate W. The values for W thus obtained are indicated by asterisks in figure 8. Generally, in the presence of energy migration over donors and energy transfer from donors to acceptors the time dependence of donor luminescence follows an initial quasi-static stage and next approaches an exponential decay $I(t) = I_0 \exp(-Wt)$. In the hopping model, the rate W is expressed as [12]

$$W = k n_a n_d \sqrt{C_{da}} \sqrt{C_{dd}} \tag{2}$$

where k is a numerical constant, n_d and n_a are the densities of donors and acceptors respectively, C_{da} and C_{dd} denote respectively a donor–acceptor interaction parameter and a donor–donor interaction parameter. The temperature dependence of W cannot be estimated because the effect of temperature on C_{da} and C_{dd} is unknown. If, for example, the C_{da} and C_{dd} depend on temperature through the phonon occupation number only, the $W(T)$ for the decay of the $^4S_{3/2}$ level would be of the form

$$W(T) = A\left[\exp(-E/kT) \Big/ \sum_i \exp(-E_i/kT)\right]^2 [\exp(E(\nu_3)/kT) - 1]^{-1} \tag{3}$$

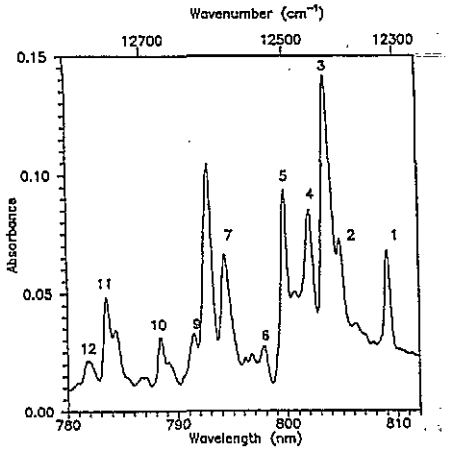

Figure 7. The absorption spectrum corresponding to the $^4I_{15/2}$–$^4I_{9/2}$ transition of Er^{3+} in $Cs_2NaErCl_{67}$ recorded at 5 K. The crystal thickness is 11 mm. See table 1 for the assignments of the lines.

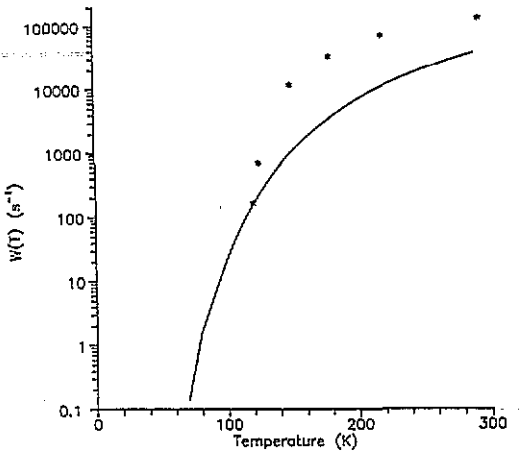

Figure 8. The influence of temperature on the $^4S_{3/2}$ luminescence quenching rate. Experimental data are indicated by asterisks. The full curve represents a fit to equation (3).

Table 1. Assignments for the $^4I_{15/2}$–$^4I_{9/2}$ absorption spectra.

Transitions	Energy (cm^{-1})	ΔE (cm^{-1})	Line No in 5 K spectrum
$a\Gamma_8$–$a\Gamma_8$	12359	0	1
$a\Gamma_8$–Γ_6+1	12425	43	2
$a\Gamma_8$–$a\Gamma_8+\nu_6$	12444	85	3
$a\Gamma_8$–Γ_6	12468	0	4
$a\Gamma_8$–Γ_6+1	12503	35	5
$a\Gamma_8$–$b\Gamma_8$	12534	0	6
$a\Gamma_8$–$\Gamma_6+\nu_4$	12589	121	7
$a\Gamma_8$–$a\Gamma_8+\nu_3$	12613	254	8
$a\Gamma_8$–$a\Gamma_8+1$	12634	275	9
$a\Gamma_8$–$a\Gamma_8+1$	12682	323	10
$a\Gamma_8$–Γ_6+1	12762	294	11
$a\Gamma_8$–$b\Gamma_8+\nu_3$	12789	257	12

Notes:
1. 1 denotes the lattice modes.
2. ΔE is the displacement from the origin.

since $n_a = n_d = n_0$ in this case. In equation (3) A comprises all factors independent of temperature; the squared factor determines the population of the $c\Gamma_8$ crystal-field level of the $^4I_{15/2}$ ground multiplet; E denotes the energy of the $c\Gamma_8$ level and the sum is performed over five crystal-field levels split out of the $^4I_{15/2}$ ground state; the last factor determines the temperature dependence of absorption of the ν_3 vibration, which fulfils the resonance condition for cross relaxation.

Putting $E = 282\ cm^{-1}$, $E(\nu_3) = 260\ cm^{-1}$ and assuming $A = 16713183$ to fit the experimental decay rate at 120 K we obtain a dependence indicated by the full curve in figure 8. This highly hypothetical dependence underestimates seriously the experimental results, but provides an order of magnitude approximation.

The rate of self-quenching of the $^4S_{3/2}$ luminescence is very high at room temperature although this process has to be assisted by phonon absorption. On the other hand, the rate of concentration quenching of Nd^{+3} luminescence in $Cs_2NaNdCl_6$ is found to be only 800 s^{-1} [6, 7] in spite of a favourable energy level scheme which allows at least two resonant transitions and several transitions involving emission or absorption of a phonon. It is clear that the energy transfer processes in $Cs_2NaLnCl_6$ are governed not only by the condition of resonance but they depend on the nature of the states or transitions involved.

The other highly efficient cross relaxation process in $Cs_2NaErCl_6$ populates the $^4F_{9/2}$ level according to the scheme

$$^2F_{5/2}(\text{site1}) + {}^4I_{15/2}(\text{site2}) \rightarrow {}^4F_{9/2}(\text{site1}) + {}^4I_{13/2}(\text{site2}) + \Delta E_{ph}$$

where ΔE_{ph} is inferior to the energy of the ν_3 vibration.

In $Cs_2NaEr_{0.2}Yb_{0.4}Y_{0.4}Cl_6$ the excitation of the $^4I_{11/2}$ level of Er^{3+} is transferred resonantly [11] to the $^2F_{5/2}$ level of Yb^{3+} according to the scheme

$$^4I_{11/2}(\text{Er}) + {}^2F_{7/2}(\text{Yb}) \rightarrow {}^4I_{15/2}(\text{Er}) + {}^2F_{5/2}(\text{Yb})$$

and is emitted exclusively by the Yb^{3+} ions, since the lifetime of the $^2F_{5/2}$ level is inferior to that of the $^4I_{11/2}$ level by roughly one order of magnitude.

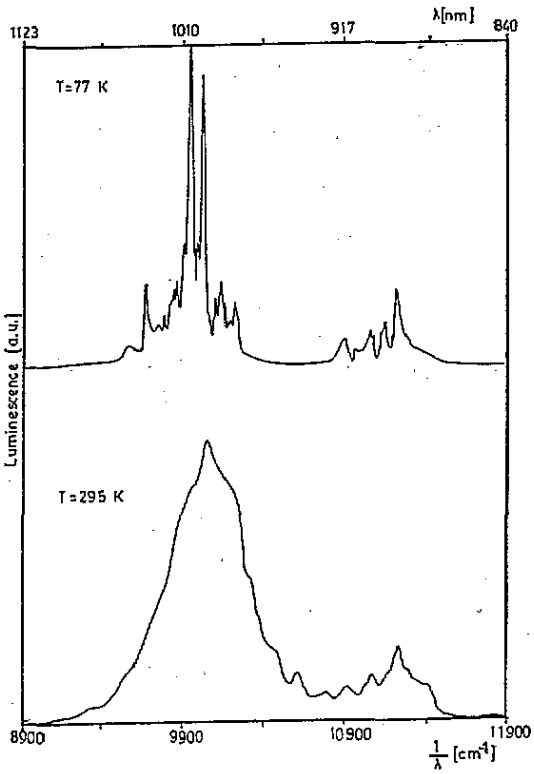

Figure 9. Luminescence spectra of $Cs_2NaNd_{0.4}Yb_{0.6}Cl_6$ at 295 and 77 K.

Another efficient energy transfer scheme is shown in figure 9 where a luminescence band is recorded with a sample of $Cs_2NaNd_{0.4}Y_{0.6}Cl_6$. The luminescence spectrum is dominated by the lines associated with the $^2F_{5/2}$–$^2F_{7/2}$ transition of Yb^{3+}, which is excited by an energy transfer from Nd^{3+} ions according to the scheme

$$^4F_{3/2}(\mathrm{Nd}) + {}^2F_{7/2}(\mathrm{Yb}) \rightarrow {}^4I_{9/2}(\mathrm{Nd}) + {}^2F_{5/2}(\mathrm{Yb}) + \Delta E_{\mathrm{ph}}.$$

Based on the reported location of the energy levels of Nd^{3+} [6] and Yb^{3+} [3] in $Cs_2NaLnCl_6$ this process meets the condition of resonance with $\Delta E_{\mathrm{ph}} \simeq 280\ \mathrm{cm}^{-1}$. It should be noted that all these efficient energy transfer processes involve transitions which strictly obey the magnetic dipole selection rules $\Delta L = 0$, $\Delta S = 0$, $\Delta J = 0, 1$. The interaction of magnetic dipoles is considered negligible [10]. On the other hand, virtually all efficient energy transfer schemes in $Cs_2NaLnCl_6$ reported to date involve transitions which obey the selection rules for a magnetic dipole transition. This is the case for Tb → Eu energy transfer [9], quenching of Eu^{3+} luminescence [10], and of Tm^{3+} luminescence [8]. Further systematic studies of the energy transfer in this lattice are needed to understand the nature and mechanism of interaction between lanthanide ions.

References

[1] Schwartz R W, Brittain H G, Riechl J P, Yeakel W C and Richardson F S 1977 *Mol. Phys.* **34** 361
[2] Morley J P, Faulkner T R, Richardson F S and Schwartz R W 1981 *J. Chem. Phys.* **75** 539
[3] Morrison C A, Leavitt R P and Wortman D E 1980 *J. Chem. Phys.* **73** 2580
[4] Jeżowska-Trzebiatowska B, Ryba-Romanowski W, Mazurak Z and Hanuza J 1980 *Chem. Phys.* **50** 209
[5] Hasan Z and Richardson F S 1982 *Mol. Phys.* **45** 1299
[6] Tofield B C and Weber H P 1974 *Phys. Rev.* B **10** 4560
[7] Stręk W, Szafrański C and Jeżowska-Trzebiatowska B 1984 *Opt. Commun.* **49** 129
[8] Foster D R, Reid M F and Richardson F S 1985 *J. Chem. Phys.* **83** 3225
[9] Bettinelli M and Flint C D 1990 *J. Phys.: Condens. Matter* **2** 8417
[10] Bettinelli M and Flint C D 1991 *J. Phys.: Condens. Matter* **3** 4433
[11] Ryba-Romanowski W, BenBouzid F, Mazurak Z, Jeżowska-Trzebiatowska B 1985 *Rare Earth Spectroscopy* (Singapore: World Scientific) p 545
[12] Voronko Y K, Osiko V V, Shcherbakov I A 1982 *Izv. Akad. Nauk SSSR, Ser. Fiz.* **46** 970
[13] Ryba-Romanowski W, Mazurak Z, Jeżowska-Trzebiatowska B 1982 *J. Lumin.* **27** 177